ANALYTICAL METHODS FOR THE STRESS CONCENTRATION ANALYSIS OF MULTILAYERED ANISOTROPIC COMPOSITES WITH ELASTIC INCLUSIONS

Werner Hufenbach, Bernd Grüber, Martin Lepper, Bingquan Zhou
Technische Universität Dresden, Institut für Leichtbau und Kunststofftechnik (ILK), 01062 Dresden, Germany

Keywords: *stress concentration, notch, elastic inclusion, multilayered composite, analytical methods*

Abstract

The problem of stress concentrations in the area of holes with elastic isotropic or anisotropic inclusions is of particular significance in the design of multilayered fibre- and textile-reinforced composite structures. For the purpose of simulating such notch zones in anisotropic multilayered composites, analytical methods offer decisive advantages since they, in comparison to numerical methods, allow weighting of influencing parameters and in this way permit a physical interpretation of complicated notch phenomena.

Sophisticated analytical solution methods for the stress concentration problem in multilayered composites with elastic inclusions were developed on the basis of layer wise solutions and have been verified by extensive experimental and numerical finite-element (FE) investigations. Finally some parameter studies and sensitivity analyses are presented.

1 Introduction

The fields of application of fibre- or textile-reinforced composite materials have been expanded considerably in recent years. While up to now the reinforcing structure mostly was constructed of uni- or bidirectional fibre-reinforced layers, textile semi-finished reinforcing products in form of multi-axial knitted, woven or braided preforms have lately been gaining increasing importance.

However, to utilize the large lightweight design potential of this group of materials, particularly in the case of future-oriented multi-material design methods, the provision of adapted calculation concepts for critical areas is indispensable. In literature (for instance in [1]-[5]) analytical solutions for the calculation of fibre-reinforced composite plates with cut-outs for various cases of geometry and loads can be found, which are mainly based on the fundamental works of LEKHNITSKII [6].

The stress concentration behaviour of cut-outs with elastic inclusions is often of great importance for the design of multilayered composites in multi-material design, since related issues occur in form of subproblems in the evaluation of rivets, screws, etc. Solutions for multilayered composites with elastic isotropic or anisotropic inclusions however are not reported very often [7], [8].

During the last years, sophisticated analytical calculation methods have been developed at the ILK for stress-concentration problems of generally structured multilayered composites (MLC) with cut-outs of different shape or for multilayer composites with circular or elliptical elastic inclusions subjected to arbitrary plate-bending and membrane loads. These methods enable a layer-by-layer pre-calculation of the entire stress and distortion field at the edge of the notch as well as in the whole plate. To have no restrictions whatsoever with regard to the composite layup it is necessary to pursue superordinate approaches in the expanded stress-deformation analysis of generally structured anisotropic multilayered composites, which also take into consideration the unfamiliar extension-bending coupling effects occurring in asymmetrical composites [9].

2 Analytical calculation methods for anisotropic plates with elastic inclusions

2.1 Plate equation

The starting point for the analysis of anisotropic multilayered composites is the HOOKE deformation law for orthotropic materials

$$\sigma_{ij} = C_{ijkl}\varepsilon_{kl} + \alpha_{ij}\Theta_{\Delta} + \beta_{ij}M_{\Delta} \qquad (1)$$

with the stresses σ_{ij}, the distortions ε_{ij} and the temperature and moisture influence $\alpha_{ij}\Theta_{\Delta}$ and $\beta_{ij}M_{\Delta}$.

In doing so the heterogeneous single layer of the composite, composed of reinforcing fibres and matrix material, is regarded as a blurred continuum by applying homogenization techniques. Based on this description of the mechanical behaviour of the single lamina, in this paper an expanded layer theory is called upon for the description of the structural behaviour of the composite. With aid of the kinematic relations,

$$\begin{bmatrix}\varepsilon_x\\ \varepsilon_y\\ \gamma_{xy}\end{bmatrix} = \begin{bmatrix}\dfrac{\partial u_0}{\partial x}\\ \dfrac{\partial v_0}{\partial y}\\ \dfrac{\partial u_0}{\partial y}+\dfrac{\partial v_0}{\partial x}\end{bmatrix} + z\begin{bmatrix}-\dfrac{\partial^2 w}{\partial x^2}\\ -\dfrac{\partial^2 w}{\partial y^2}\\ -2\dfrac{\partial^2 w}{\partial x\partial y}\end{bmatrix} = \begin{bmatrix}\varepsilon_x^0\\ \varepsilon_y^0\\ \gamma_{xy}^0\end{bmatrix} + z\begin{bmatrix}\kappa_x\\ \kappa_y\\ \kappa_{xy}\end{bmatrix} \qquad (2)$$

associating the displacements of the neutral plane u_0, v_0 and w_0 in x-, y-, z-direction with the strains ε_x, ε_y, γ_{xy} and curvatures κ_x, κ_y, κ_{xy}, the structural law for multilayered composites is derived, taking into consideration thermal- and media-related influences

$$\begin{bmatrix}N_x\\ N_y\\ N_{xy}\\ M_x\\ M_y\\ M_{xy}\end{bmatrix} = \begin{bmatrix}A_{11} & A_{12} & A_{16} & B_{11} & B_{12} & B_{16}\\ A_{12} & A_{22} & A_{26} & B_{12} & B_{22} & B_{26}\\ A_{16} & A_{26} & A_{66} & B_{16} & B_{26} & B_{66}\\ B_{11} & B_{12} & B_{16} & D_{11} & D_{12} & D_{16}\\ B_{12} & B_{22} & B_{26} & D_{12} & D_{22} & D_{26}\\ B_{16} & B_{26} & B_{66} & D_{16} & D_{26} & D_{66}\end{bmatrix} \cdot \begin{bmatrix}\varepsilon_x^0\\ \varepsilon_y^0\\ \gamma_{xy}^0\\ \kappa_x\\ \kappa_y\\ \kappa_{xy}\end{bmatrix} - \begin{bmatrix}N_x^T\\ N_y^T\\ N_{xy}^T\\ M_x^T\\ M_y^T\\ M_{xy}^T\end{bmatrix} - \begin{bmatrix}N_x^Q\\ N_y^Q\\ N_{xy}^Q\\ M_x^Q\\ M_y^Q\\ M_{xy}^Q\end{bmatrix} \qquad (3)$$

(A_{ij}), (B_{ij}), (D_{ij}): extensional, extension-bending coupling and bending stiffnesses of multilayered composites,

ε^0_i, γ^0_{ij}, κ_k: distortions of the neutral plane,

N_i, M_i^T, N_i^Q, M_i^Q: thermal-related or media-induced force resultants and moment resultants.

In multilayered fibre-reinforced composite materials, due to coupling of force resultants and curvatures as well as coupling of moment resultants and strains occurring in asymmetrical composites, a separation of the plate-bending and membrane problems often is not possible. Therefore, expanding on the classic plate theory by KIRCHHOFF, the formulation of the equilibrium of force and moment resultants at the differential plate element is supplemented by the membrane force resultants. A generalizing plate equation is derived from these expanded equilibrium equations, which in particular considers the above described coupling effects in asymmetric composites (see also [10], [11]). The partial differential equation system (PDES) of this generalizing plate equation can be written down by means of a differential operator matrix in compact and clear form as a matrix equation, which uses the expanded structural law for multilayered composites (3).

$$\underline{\underline{\Delta}}\begin{bmatrix}(A_{ij}) & (B_{ij})\\ (B_{ij}) & (D_{ij})\end{bmatrix}\underline{\underline{\Delta}}^T\begin{bmatrix}u_0\\ v_0\\ w_0\end{bmatrix} = -\underline{\underline{\Delta}}\begin{bmatrix}(N_i)\\ (M_i)\end{bmatrix} + \underline{\underline{\Delta}}\left(\begin{bmatrix}(N_i^T)\\ (M_i^T)\end{bmatrix} + \begin{bmatrix}(N_i^Q)\\ (M_i^Q)\end{bmatrix}\right) \qquad (4)$$

with

$$\underline{\underline{\Delta}}^T = \begin{bmatrix}\dfrac{\partial}{\partial x} & 0 & \dfrac{\partial}{\partial y} & 0 & 0 & 0\\ 0 & \dfrac{\partial}{\partial y} & \dfrac{\partial}{\partial x} & 0 & 0 & 0\\ 0 & 0 & 0 & -\dfrac{\partial^2}{\partial x^2} & -\dfrac{\partial^2}{\partial y^2} & -2\dfrac{\partial^2}{\partial x\partial y}\end{bmatrix} \qquad (5)$$

u_0, v_0, w_0: displacements of the neutral plane,

P: vector of external loads.

This physically illustrative and well manageable formal representation of the well known PDES (see for example [12]-[14]) was first given by Lepper [15].

2.2 Complex-valued displacement functions and method of conformal mapping

For the further investigations, an infinite plate with a finite elliptical or circular elastic inclusion is selected as mathematical equivalent. To determine solutions for the PDES of the plate equation (4) the system is equivalently converted into a single differential equation in of eighth-order. Applying the method of complex-valued displacement functions as an extension of the method of complex-valued stress functions, which is well established in plane theory of elasticity, the solution of the generalized plate equation (4) can be written in the form

$$w_0 = 2\,\mathrm{Re}\left(\sum_{k=1}^{4} r_k \Psi_k(\zeta_k)\right) \qquad (6)$$

with four analytical functions $\Psi_k(\zeta_k)$ referring to the four different complex planes $\zeta_k = \zeta + \lambda_k\bar{\zeta}$ and $\zeta = x + iy$. The complex parameters λ_k are calculated as roots of the characteristic equation, which results from inserting (6) into the converted differential equation in w_0 arising from (4). Since, in the case of real

materials, it can be shown, that from the eight different roots of the characteristic equation always two by pairs have to be conjugated complex, only four independent roots have to be taken into account in (6).

For the effective handling of boundary conditions for the stress concentration problem, the notched area is projected onto the exterior of a unit circle using the method of conformal mapping. This opens the possibility of a uniform approach for the determination of the respective displacement functions, independently of the actual notch contour. In this special case the conformal mappings of the unit circle E in the ζ-plane onto the area of the plate S in the ϑ-plane and the assigned affinely distorted areas $S^{(k)}$ in the respective ϑ_k-planes are determined, where the points A, $A^{(1)}$,…, $A^{(4)}$, which are assigned to each other by the affine projections, must have the same pre-image A_ζ on the edge of the unit circle E (Fig. 1) [16].

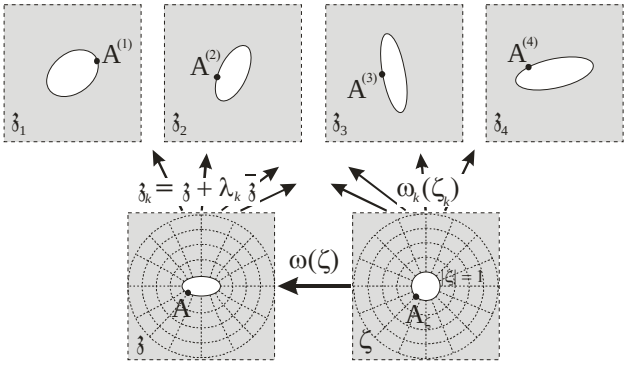

Fig. 1. Conformal mappings of the ζ-plane onto the ϑ- and ϑ_k-planes

In the case of circular or elliptical notches, which are covered by this publication, these mappings result from

$$\vartheta = \omega(\zeta) = \frac{a+b}{2}\zeta + \frac{a-b}{2}\frac{1}{\zeta}, \tag{7}$$

$$\vartheta_k = \omega_k(\zeta_k) = \left(\frac{1+\lambda_k}{2}a + \frac{1-\lambda_k}{2}b\right)\zeta_k + \left(\frac{1+\lambda_k}{2}a - \frac{1-\lambda_k}{2}b\right)\frac{1}{\zeta_k} \tag{8}$$

with $\zeta \equiv \zeta_k$ and a, b as the semi-axes of the elliptical notch.

2.3 Boundary conditions

For the solution of the respective boundary value problem, the complex valued displacement functions and with this the analytical functions Ψ_k in (6) have to be adapted to the boundary conditions. In order to take into consideration not only the effects resulting from the elastic inclusion but as well additional technically relevant external loads, the actual state of stress is decomposed using the superposition principle as follows (see as well Fig. 2):

- **I** a notched plate loaded on the outer and inner boundary
- **Ia** a finite, unnotched plate with loads on the outer edge
- **Ib** an infinite, notched plate with loads at the edge of the notch, adapted in such a way that, with superposition of **Ia** and **Ib**, an overall unloaded notch edge results,
- **Ic** an infinite notched plate with the corresponding loads from **I** at the notch edge,
- **II** a finite elastic inclusion loaded at the outer boundary.

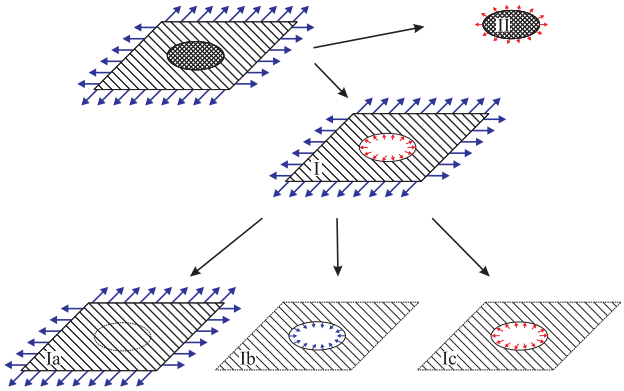

Fig. 2. Decomposition of the coupled membrane-plate problem by means of superposition

With aid of this decomposition of the problem it is possible to take into consideration the dynamic boundary conditions on free boundaries, resulting from technically relevant external loads at the outer boundary (Fig. 3a)

$$\tilde{N}_n^0, \tilde{N}_t^0, \tilde{M}_n^0, \tilde{Q}_E^0 = \tilde{Q}^0 + \frac{d\tilde{M}_t^0}{ds_0} \tag{9}$$

and the transition condition on the edge between surrounding plate and elastic inclusion (Fig. 3b)

$$\tilde{N}_n = -\tilde{N}_n^e, \tilde{N}_t = -\tilde{N}_t^e, \tilde{M}_n = -\tilde{M}_n^e,$$
$$\tilde{Q} + \frac{d\tilde{M}_t}{ds} = -\left(\tilde{Q}^e + \frac{d\tilde{M}_t^e}{ds}\right), \tag{10}$$
$$u = u^e, v = v^e, \frac{\partial w}{\partial x} = \frac{\partial w^e}{\partial x}, \frac{\partial w}{\partial y} = \frac{\partial w^e}{\partial y}.$$

For dealing with the subproblem **II** (the elastic inclusion, see Fig. 2), an adapted approach for a displacement function is chosen

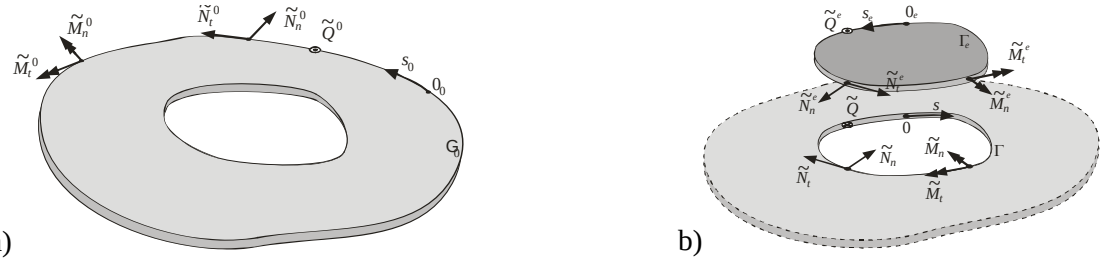

a) b)

Fig. 3. Boundary and transition conditions for multilayered anisotropic plates with elastic inclusions
a) dynamic boundary conditions on free outer edges of the plate
b) dynamic and kinematic transition conditions on the edge between plate and inclusion

$$
\begin{aligned}
u^e &= P_1^e x + P_2^e y + Q_1^e x^2 + U_{xy}^e xy + Q_2^e y^2 + C_3^e y + C_1^e,\\
v^e &= P_2^e y + P_3^e x + Q_3^e x^2 + V_{xy}^e xy + Q_4^e y^2 - C_3^e x + C_2^e,\\
w^e &= P_4^e x^2 + P_5^e xy + P_6^e y^2 + Q_5^e x^3 + Q_6^e x^2 y + Q_7^e xy^2\\
&\quad + Q_8^e y^3 + C_4^e y + C_5^e x + C_6^e.
\end{aligned}
\tag{11}
$$

By complex Laurent series expansion, a comparison of coefficients on the edge between plate and inclusion and an additional boundary condition corresponding to the requirement of the existence of a reference point, a linear system of 39 equations for the 39 unknowns is to be determined.

3 Experimental and numerical FE-verification

For the verification of the developed calculation methods for multilayered composites with elastic inclusions, extensive experimental and numerical finite-element (FE) investigations have been carried out. These comparative studies have been conducted on multilayered composites build from carbon-fibre reinforced polymer (CFRP) UD-layers (parameters: $E_{\parallel}$ = 135 GPa, $E_{\perp}$ = 8.2 GPa, $G_{\parallel\perp}$ = 4.7 GPa, $\nu_{\parallel\perp}$ = 0.3) with different lay-ups.

Representative results are presented here from the large number of experimental and numerical investigations.

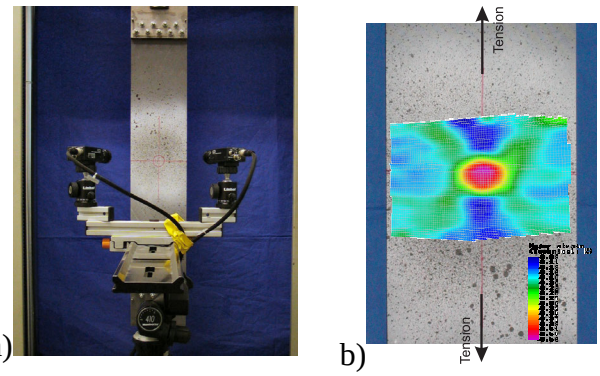

a) b)

Fig. 4. Grey-scale measurement of a $[+30/-30]_s$-CFRP-plate with elastic PU-inclusion
a) experimental set-up
b) grey-scale results (major strains)

3.1 Experimental results

In Fig. 4a the experimental set-up is shown, where a MLC-plate with an elastic PU-inclusion is statically loaded in a tension test. Thereby the grey-scale correlation method (GCM) as modern 3D-field measurement method is applied for the determination of the displacement- and strain-fields (Fig. 4b).

As an example in Fig. 5 a comparison of the analytically calculated and experimentally determined decay behaviour of ε_x- and ε_y-strains on the 0°-radian (direction of tension) and the 90°-radian (perpendicular to the direction of tension) is presented. The diagram shows the good correlation between experimental and analytical results.

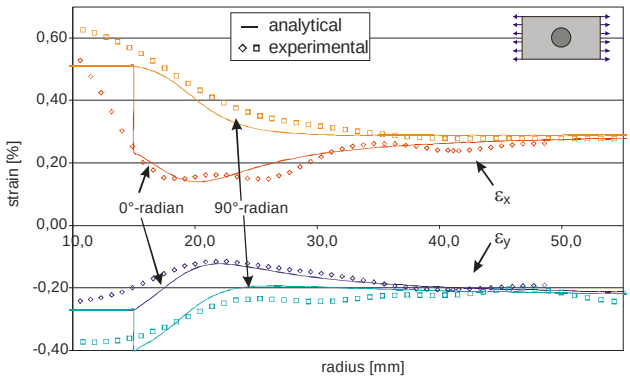

Fig. 5. Comparison of the strain decay behaviour for a $[+45/-45]_s$-CFRP-plate with elastic PU-inclusion under unidirectional N_x tension load

3.2 Numerical (FE) results

To reduce the number of complex experimental investigations, a large number of FE-calculations on different MLCs with isotropic and anisotropic inclusions and different loading-combinations on the outer boundary have been carried out. Fig. 6 shows an example for the FE-model of a MLC-plate with an elliptical elastic inclusion, loaded by pure shear-forces on the outer boundary. In addition, to inhibit rigid body motions, the translative and rotatory de-

grees of freedom are blocked for one node in the centre of the inclusion.

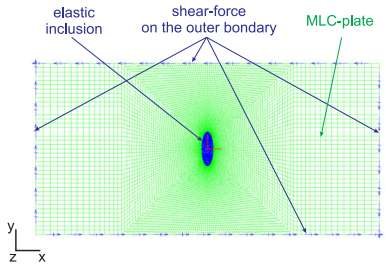

Fig. 6. MLC-plate with an elliptical elastic inclusion, loaded under pure shear-forces load

As representative results, in Fig. 7 a comparison of the analytically and numerically calculated decay behaviour of the distortions along the 0°-radian of a symmetric $[+45/-45]_s$-CFRP-plate with an isotropic elliptical Al-inclusion is presented. The plate is loaded under unidirectional tension in x-direction. For all distortions ε_x, ε_y and γ_{xy} a very good correlation of the numerical and the analytical results is observed.

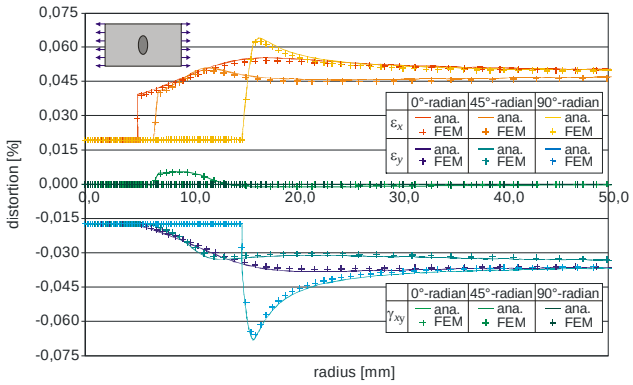

Fig. 7. Comparison of the distortion-decay behaviour in 0° direction for a $[+45/-45]_s$-CFRP-plate with elliptical elastic Al-inclusion under unidirectional N_x tension load

As a second example a comparison of the decay behaviour of the distortions along the 0°-radian of an unsymmetric [+45/-45]-CFRP-plate with a symmetric $[+45/-45]_s$-CFRP-inclusion is presented in Fig. 8. The plate is loaded with uniform tension in x- and y-direction. The distortions have been calculated and compared for the laminate top and laminate bottom.

For this example again a very good correlation of the numerically obtained and the analytically calculated distortion values ε_x, ε_y and γ_{xy} on the laminate top and bottom is observed. Such a very good correlation can be observed for all problems

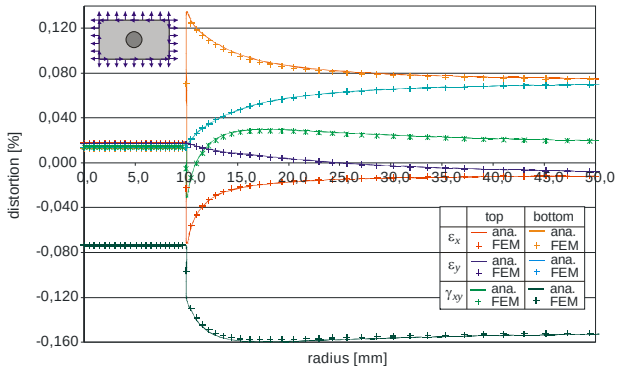

Fig. 8. Comparison of the distortion-decay behaviour in 0° direction for a [+45/-45]-CFRP-plate with an elastic $[+45/-45]_s$-CFRP-inclusion under combined N_x, N_y tension and N_{xy} shear load

concerning unsymmetric composites, which have been assayed. This outlines in an impressive way, that the developed calculation method is applicable for the whole field of symmetric and unsymmetric composites under pure or combined plate-bending and membrane loadings.

3.3 Conclusions from the experimental and numerical investigations

The acquired experimental results as well as the numerical results established by the finite-element method show a good correlation with the pre-calculated analytical solutions and thus endorse the developed theory in an impressive way. Based on this strong support, the developed calculation methods offer a very good basis for the development of new fast dimensioning-tools for the end-user dealing with multilayered unidirectional or textile-reinforced composites with elastic inclusions. The method is not only applicable for symmetric composites but as well includes the influences of the extension-bending coupling and therefore can be used for unsymmetric composites as well. This is of great importance, since unsymmetric composites are more and more often used in industrial application.

4 Parameter studies on multilayered composites with elastic inclusions

The newly developed analytical methods for the stress concentration analysis of MLC with elastic inclusions show their great potential in the case of systematic and fast parameter studies and sensitivity analysis. Furthermore, their physical transparency provides the opportunity to interpret the occurring and sometimes unusual effects. Therefore the developed methods have been implemented in fast and easy to use computer programs.

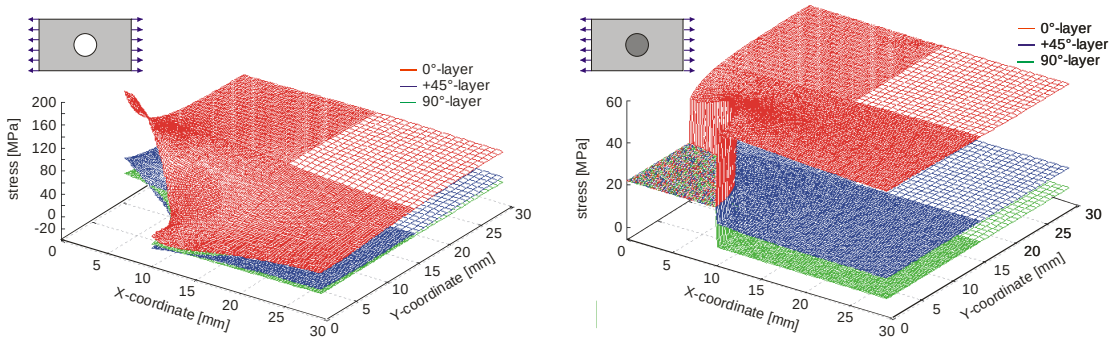

(a) without inclusion (b) with elastic Al-inclusion

Fig. 9. Comparison of the σ_x-stress-fields for a multilayered $[0/+45/-45/90]_s$-CFRP-plate with and without elastic inclusion under tension load N_x = 40 N/mm

4.1 Comparison of notched plates with and without inclusion

As a first example for the use of the developed method a comparison of the stress-fields of a notched $[0/+45/-45/90]_s$-CFRP-plate with elastic Al-inclusion and without inclusion is presented. The plate is loaded with uniaxial tension in x-direction N_x = 40 N/mm. The diameter of the hole and the inclusion is ∅ = 20 mm.

Fig. 9 shows a comparison of the σ_x-stress-fields for different layers of the composite. It can be observed, that in both cases the stress-values are of the same size in a sufficient distance from the inclusion and the hole respectively. On the other hand, in the area of the disturbance the σ_x-layer-stresses in the 0°-layer for the plate without inclusion reach the height of 155 MPa while in the plate with elastic Al-inclusion the stresses are considerably lower. This effect can be observed for all layers. In the case presented here, the elastic Al-inclusion leads to an overall reduction of the stress concentrations.

In addition this example demonstrates once again, that for dimensioning multilayered composites a layer by layer analysis of the stress- and strain-fields is of great importance.

4.2 Sensitivity analysis on the size of the inclusion

In a second example, the influence of the dimension of the elastic inclusion on the layer wise stress-concentration-field is studied. Fig. 10 shows the diagrams for a symmetric $[0/+45/-45/90]_s$-CFRP multilayered composite with different inclusion diameters under unidirectional tension loading in x-direction N_x = 60 N/mm. As inclusion-material Aluminum was chosen. The selected layerwise diagrams in Fig. 10 show only the dominating stress for the layers, i. e. the σ_x-stress for the 0°-layer (Fig. 10 (a)) and the σ_y- stress for the 90°-layer (Fig. 10 (b)).

From the presented results it can be seen, that the stress-concentration directly at the edge between inclusion and surrounding plate is independent on the size of the inclusion. In contrast to this independency on the size, the decay behaviour of the stresses clearly depends on the size of the inclusion. In sufficient distance of the inclusion the disturbance of the stress-field has decayed, as can bee seen from Fig.

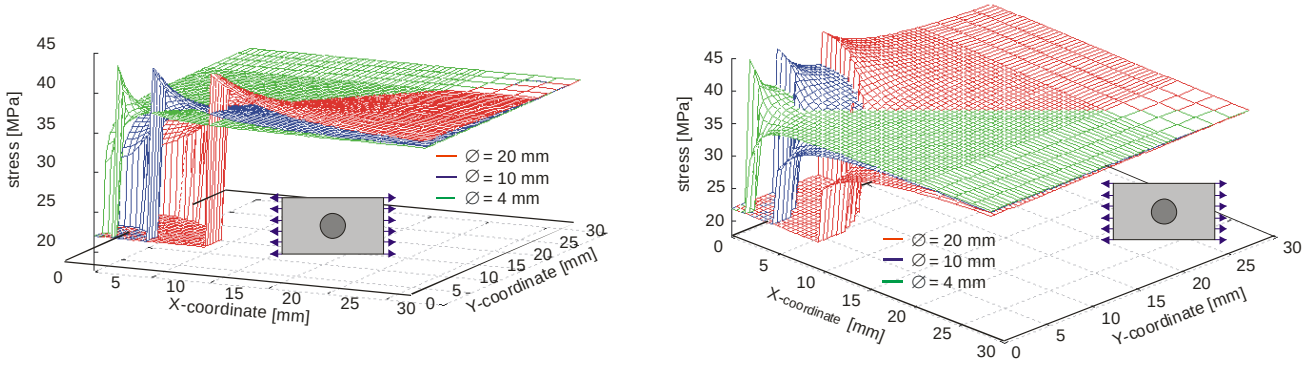

(a) σ_x-stress for the 0°-layers (b) σ_y-stress for the 90°-layers

Fig. 10. Layerwise decay behaviour of selected stresses in a $[0/+45/-45/90]_s$-CFRP MLC depending on the diameter of the Al-inclusion under tension load N_x = 60 MPa

10. The size of this area and especially the gradient of the decrease of the size-influence varies with the diameter of the inclusion: The bigger the size of the inclusion the greater the area where the influence is significant and the lower the gradient of the decrease. This underlines once more, that for realistic strength criteria for notched MLC not only the absolute values of the stress concentrations directly at the edge of the notch / inclusion should be considered, but as well the decay characteristics should be taken into account, as it is done in the point-stress-criteria or the average-stress-criteria, which reflect the so called "microsupport" effect according to NEUBER [21] without mentioning it explicitly.

4.3 Parameter study on the influence of the orientation of the inclusion

As a final example a parameter study on the influence of the orientation of an anisotropic elastic inclusion on the stress-concentration field is presented. As object of this study a symmetric $[+45/-45]_s$-CFRP MLC-plate is chosen with an anisotropic inclusion made from the same material. The orientation of the inclusion is rotated around the z-axis, so it varies with regard to the orientation of the plate. In the example a pure unidirectional tension load in 0°-direction and a plate bending load are applied (Fig. 11).

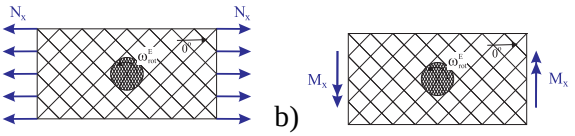

a) b)

Fig. 11. Models for the parameter study on the inclusion orientation
a) tension loading N_x
b) plate bending M_x

In Fig. 12 the layer σ_x-stresses are presented exemplarily for this parameter variation. For inclusion orientations of 0° and 180° the laminate of the MLC-plate and the inclusion have the same orientation. For these orientations an undisturbed plate is dealt with from a macroscopic point of view since the model is based on the assumption of perfect adhesion between plate and inclusion. In the diagrams Fig. 12 a) and Fig. 12 b) this is reflected by the fact, that the stresses are constant along the notch boundary.

In case of the tension load starting from the constant stresses for the orientation $\omega_{rot}^{E} = 0°$ a significant increase of the maxima of stresses over the notch boundary orientation is observed with increasing ω_{rot}^{E} until for an orientation of 45° the absolute extremal stress-values are reached. For the orientation of 45° the direction of the maximal E-modulus of the inclusion are 0° and 90° and thus are parallel to the directions of the minimal E-modulus of the MLC-plate. With a further increasing angle $45° < \omega_{rot}^{E} \leq 90°$ the extrema of the stresses decrease until for $\omega_{rot}^{E} = 90°$ the stresses are again constant over the notch boundary coordinate. For the orientation of 90° the directions of the maximal E-modules of the inclusion and the MLC-plate are parallel again. Since the composite is regarded as a continuum homogenized over the thickness, in the case of pure membrane loads the orientation of 90° is equivalent to the orientation of 0°. Thus the further stress distribution for $90° < \omega_{rot}^{E} \leq 180°$ can be obtained by reflection on a plane through $\omega_{rot}^{E} = 90°$.

For the plate bending load the behaviour is different. Of course the stresses for $\omega_{rot}^{E} = 0°$ and $\omega_{rot}^{E} = 180°$ are constant over the notch boundary coordinate. But since the stacking sequence of the composite has great influence in the case of bending

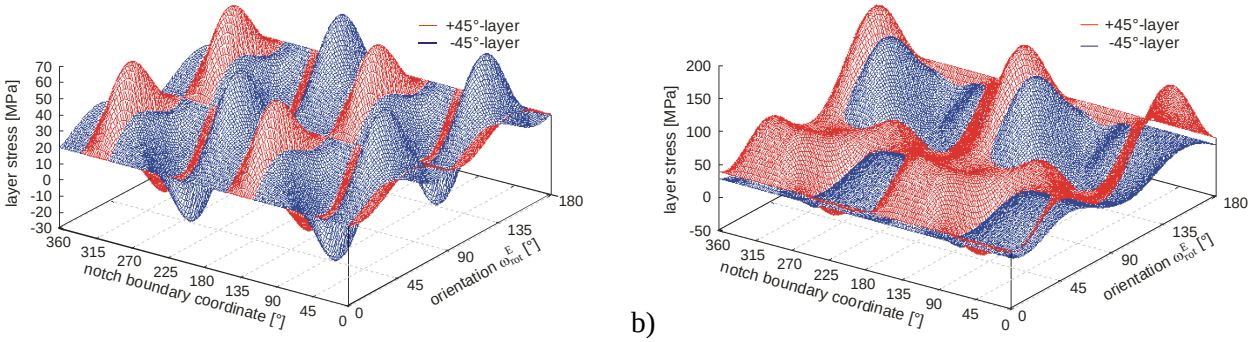

a) b)

Fig. 12. σ_x-layer-stresses for the variation of the inclusion orientation ω_{rot}^{E}
a) tension loading
b) plate bending

loads, no further symmetry is observed, especially the orientation $\omega_{rot}^{E} = 90°$ is not equivalent to $\omega_{rot}^{E} = 0°$.

5 Conclusions

For the problem of multilayered composites with elastic isotropic or anisotropic inclusions examined here, analytical solution methods based on complex valued displacement functions and the method of conformal mapping have been developed. Here, we should emphasize that not only stresses, distortions and displacements directly at the edge of the notch can be calculated, but also their distribution throughout the entire plate. Experimental investigations have been carried out, which show a very good correlation of the measured and the calculated results. Additionally a vast number of FE calculations were performed with symmetrical and unsymmetrical composite structures for further verification of the developed calculation methods. A comparison of these numerically obtained values and the results obtained by means of the developed analytical solutions also showed a high level of congruence. Especially it was proved, that the developed calculation method is applicable for the whole field of symmetric and unsymmetric composites, taking into account the material induced coupling of the plate-bending and the membrane problem.

The performed parameter studies demonstrate that very complex mechanisms are acting in MLC plates in the area of holes with elastic inclusions Therefore, in the interest of dimensioning structures weakened by elastic inclusions in line with material and component characteristics, a precise layer-by-layer analysis of the distribution of stresses and distortions is absolutely indispensable. Starting from this layer-by-layer approach with additional consideration of so called physically based failure criteria, for instance, according to PUCK [17]-[19] or CUNTZE [20] and under additional consideration of the so-called microsupport effect according to NEUBER [21], the development of new failure criteria for notched multilayered composites is currently one of the focal points of ongoing research work at the ILK [22].

Acknowledgements

We would like to express our gratitude towards the Deutsche Forschungsgemeinschaft (DFG), who is funding the subproject B2 within the scope of SFB 639 “Textile-Reinforced Composite Components in Function-Integrating Multi-Material Design for Complex Lightweight Applications”.

References

[1] Konisch H. J., Whitney J.M. “Approximate stresses in an orthotropic plate containing a circular hole”. *Journal of Composite Materials*, Vol. 9, pp 157-167, 1975.

[2] Hwu C., Ting T. C. T. “Two-dimensional problems of the anisotropic elastic solid with an elliptic inclusion”. *Q. Jl. Mech. Appl. Math.*, Vol. 42, pp 553-572, 1989.

[3] Ukadgaonker V. G., Rao D. K. N. “A general solution for stresses around holes in symmetric laminates under inplane loading”. *Composite Structures*, Vol. 49, No. 2, pp 339-354, 2000.

[4] Ukadgaonker V. G., Rao D. K. N. “A general solution for stress resultants and moments around holes in unsymmetric laminates”. *Composite Structures*, Vol. 49, No. 1, pp 27-39, 2000.

[5] Hufenbach W., Kroll L., Langkamp A., Lepper M., Werdermann B. “Advanced calculation method for notched textile-reinforced hybrid composites”. *12th International Conference on Mechanics of Composite Materials (MCM 2002)*, Riga (Latvia), 09.-13. July 2002.

[6] Lekhnitskii S. G. “*Anisotropic Plates*”. Transl. 2nd russ. print run: S. W. Tsai and T. Cheroin, New York et al.: Gordon and Breach, 1968.

[7] Engels H., Becker W. “Closed-form analysis of external patch repairs on laminates”. *Composite Structures*, Vol. 56, No. 3, pp 259-268, 2002.

[8] Zhou B. „*Beitrag zur Berechnung endlich berandeter anisotroper Scheiben mit elastischem Einschluss*“. PhD-Thesis, TU Clausthal, 1997.

[9] Grüber B. “*Beitrag zur Strukturanalyse von anisotropen Schichtverbunden mit elastischen Einschlüssen und Bolzen*”. PhD-Thesis, TU Dresden, 2004.

[10] Hufenbach W., Kroll L., Langkamp A., Lepper M., Werdermann B. “Theoretische und experimentelle Kerbspannungsanalyse bei Textil-Holz-Mehrschichtverbunden mit Inserts“. *Proceedings of the 2nd Colloquium on Textile-Reinforced Structures (CTRS 2)*, Dresden, pp 259-271, 29.09.-01.10. 2003.

[11] Hufenbach W., Grüber B., Langkamp A., Lepper M., Kroll L.“Advanced calculation methods for notched hybrid composites with textile-reinforced polymers”. *Journal of Plastics Technology*, Vol. 3 No. 2, 2007.

[12] Altenbach H., Altenbach J., Rikards R. “*Einführung in die Mechanik der Laminat und Sandwichtragwerke: Modellierung und Berechnung von Balken und Platten aus Verbundwerkstoffen*“.

Stuttgart: Dt. Verl. für Grundstoffindustrie, 1996.

[13] Reddy J. N. "*Mechanics of laminated composite plates: theory and analysis*". Boca Raton et al.: CRC Press, 1996.

[14] Becker W. "Complex method for the elliptical hole in an unsymmetric laminate". *Archive of Applied Mechanics*, Vol. 63, pp 159-169, 1993.

[15] Lepper M. "*Kerbspannungsanalyse anisotroper Mehrschichtverbunde mit symmetrischem und unsymmetrischem Strukturaufbau*". PhD-Thesis, TU Clausthal, 1999.

[16] Grüber B., Hufenbach W., Kroll L., Lepper M., Zhou B. "Stress concentration analysis o fibre-reinforced multilayered composites with pin-loaded holes". *Composites Science and Technology*, Vol. 67, pp 1439-1450, 2007.

[17] Hashin Z. "Failure Criteria for Unidirectional Fibre Composites." *Journal of Applied Mechanics*, Vol. 47, pp 329-334, 1980.

[18] Puck A. "*Festigkeitsanalyse von Faser-Matrix-Laminaten: Modelle für die Praxis*". München Wien: Carl Hanser Verlag, 1996.

[19] Puck A., Schürmann H. "Failure analysis of FRP laminates by means of physically based phenomenological models". *Composite Science and Technology*, Vol. 58, No. 7, pp 1045-1067, 1998.

[20] Cuntze R. G., Freund A. "The predictive capability of failure mode concept-based strength criteria for multidirectional laminates". *Composites Science and Technology*, Vol. 64, No. 3/4, pp 343-377, 2004.

[21] Neuber H. "*Kerbspannungslehre*". Berlin et al.: Springer-Verlag, 2001.

[22] Kroll L, Lepper M, Grüber B, Kostka P, Zhou B. "Analytical models for stress and failure analysis". in: *Proceedings of the 21st International Congress of Theoretical and Applied Mechanics (ICTAM-21)*, Warschau, p. 298, 15.-21.8.2004.